JOURNAL OF AGRICULTURAL AND FOOD CHEMISTRY

Article

pubs.acs.org/JAFC

Investigating the Thermal Decomposition of Starch and Cellulose in Model Systems and Toasted Bread Using Domino Tandem Mass Spectrometry

Agnieszka Golon,[†] Francisco Javier González,[§] Juan Z. Dávalos,[§] and Nikolai Kuhnert*[,†]

[†]School of Engineering and Science, Jacobs University Bremen, Campus Ring 1, 28759 Bremen, Germany

[§]Instituto de Quimica Fisica Rocasolano, CSIC, Serrano 119, 28006 Madrid, Spain

Supporting Information

ABSTRACT: Many dietary products containing polysaccharides, mostly starch and cellulose, are processed by thermal treatment. Similarly to the formation of caramel from mono- and disaccharides, the chemical structure of the carbohydrates is dramatically altered by heat treatment. This contribution investigates the products of thermal decomposition of pure starch and cellulose as model systems followed by an investigation of bread obtained at comparable conditions using a combination of modern mass spectrometry techniques. From both starch and cellulose, dehydrated oligomers of glucose and dehydrated glucose have been predominately observed, with oligomers of more than four glucose moieties dominating. Moreover, disproportionation and oligomers with up to six carbohydrates units are formed through unselective glycosidic bond breakage. MALDI-MS data confirm the presence of the majority of products in toasted bread.

KEYWORDS: *browning, starch, cellulose, complex mixtures, mass spectrometry*

INTRODUCTION

Carbohydrates, the most abundant biomolecules in nature, are present in all living system as monosaccharides or combined as polysaccharides,[1] playing an important role as structural material and energy reserves.[2] All foods of plant origin contain polysaccharides in abundance. Starch and cellulose are the two most common polysaccharides present in dietary plants, consisting of glucose connected via α-1,4- and β-1,4-glycosidic bonds, respectively.[3] In particular, starch is observable in various dietary plant sources (e.g., corn, potato, wheat, and rice)[4,5] being the most important source of chemical energy in food as well as the predominant contributor to energy intake in a typical human diet.[6−8]

Most foods are consumed by humans after thermal treatment including cooking, baking, frying, or roasting. In the process of these thermal treatments all carbohydrates in food undergo significant chemical changes frequently described as non-enzymatic browning reactions. In the field of carbohydrate chemistry the best-known examples are the thermal conversion of glucose and sucrose to caramel and the Maillard reaction between saccharides and amino acids at elevated temperatures, forming a material referred to as melanoidins. Melanoidins are present in all thermally treated carbohydrate-rich foods with their daily human intake from all dietary sources estimated by Fogliano and Morales at 10 g per day.[9] Melanoidins are composed of reaction products arising from thermal treatment of carbohydrates alone and from reaction products of carbohydrates with nitrogen-containing species including amino acids and proteins. Despite many advances, the molecular composition of melanoidins and the mechanism of formation of thermally treated carbohydrates must be considered as sketchy. This fact is closely linked to the limitations of analytical chemistry, which in the past, due to restrictions in resolving power, has struggled to provide methods capable of analyzing extremely complex materials containing thousands of individual analytes.

Recently, modern mass spectrometry has evolved as a technique able to overcome these limitations and provide for the first time detailed insight into the myriad compounds formed in food processing providing both structural information and mechanistic information. We have developed an analytical strategy, which we have termed domino tandem mass spectrometry. In a first step we take advantage of the ultimate resolving power of ultrahigh-resolution mass spectrometry (MS) to count all detectable analytes within the sample and provide extensive lists of molecular formulas present in the sample. Using graphical and chemometric tools such as van Krevelen analysis, Kendrick analysis, or homologous series analysis, the experimental data set is exploited to establish a structural and mechanistic model accounting for all chemical processes in the sample. In a second consecutive step (therefore the term domino tandem) using LC-tandem MS, the structural hypothesis is verified or not. Using LC-tandem MS, it is possible to resolve isomeric compounds in the chromatographic dimension and obtain valuable structural information based on fragment spectra. We have applied this approach to the analysis of black tea thearubigin formation,[10] to the formation of roasted coffee melanoidins,[11] and recently to the investigation of caramel formed from glucose, fructose, and sucrose.[12] In this contribution we apply our analytical strategy to the investigation of thermal decomposition products obtained

Received: May 16, 2012
Revised: October 27, 2012
Accepted: December 20, 2012
Published: December 20, 2012

from starch and cellulose model systems followed by an investigation on thermal degradation products in toasted bread as a real food example, thereby identifying a large series of compounds structurally identical to those formed in the model systems.

Besides the important area of food chemistry, thermal treatment of polysaccharides is used in many other industries,[13] including products such as paper, adhesives, cosmetics, bioplastics, and, most importantly, biofuel.[14] Cellulose is the main cell wall polysaccharide,[15] and the most abundant biological material on Earth,[16] with production of approximately 1.5×10^{12} tons annually.[17] In particular, the production of biofuels from cellulose-rich agricultural plants takes frequent advantage of thermal processing steps to achieve carbonization, including steps chemically identical to those observed in baking or roasting.

MATERIALS AND METHODS

Chemicals. All solvents (analytical grade) and chemicals were purchased from Sigma-Aldrich (Bremen, Germany).

Sample Preparation. All sugar samples (1 g) were heated in an oven for 2 h at 180 °C (glucose) and 220 °C (starch and cellulose). The heated samples were stored at room temperature. Heated carbohydrates (1 mg) were dissolved in water, filtered, and directly used for mass spectrometry measurements. Toast was prepared from bread purchased from a supermarket in Bremen, Germany. The slices of bread were heated in the toaster for 3 min. Afterward, the crust was removed and dissolved in water for analyses.

ESI-FT-ICR MS. ESI-FT-ICR experiments were performed on a high-resolution mass spectrometer FT-ICR (Fourier Transform Ion Cyclotron Resonance) Varian-920, provided with a 7.0 T actively shielded superconducting magnet and equipped with an ESI source in line with a triple-quadrupole Varian-320 MS. The solution was directly infused into the ESI source at 20 μL/min of the flow rate. Quadrupole and hexapole ion guides, accumulation ion hexapole, and the other key components were optimized to maximize detection in the m/z 200–1500 range. Commercial beer maltooligosaccharides were used as mass calibrants and tuning standards in both positive and negative ion modes.[18] Tandem MS experiments were performed pulsing a 10.6 μm CO_2 laser (Synrad model 48-2, Mukilteom WA, USA) for infrared multiphoton dissociation (IRMPD). Product ion formation was optimized by varying the IRMPD laser pulse around 400 ms at ~45% of total power (25 W).

High-Resolution ESI-TOF-MS. High-resolution mass spectra were recorded using a Bruker Daltonics micrOTOF instrument employing negative and positive electrospray ionization modes. The MicrOTOF Focus mass spectrometer (Bruker Daltonics) was fitted with an ESI source, and internal calibration was achieved with 10 mL of 0.1 M sodium formate solution. Calibration was carried out using the enhanced quadratic calibration mode. All MS measurements were performed in negative and positive ion modes. It should be noted that the intensities of the measured peaks in a TOF calibration, influenced the magnitude of the mass error with high-intensity peaks resulting in detector saturation displaying larger mass errors. Usually this problem can be overcome by using spectra averaging on the side flanks of a chromatographic peak or by taking more diluted samples.

Data Analysis. Molecular formulas were calculated using Bruker software Data Analysis 4.0. The data were subsequently exported to Excel to carry out a simple mathematical operation such as determination of H/C and O/C ratios or Kendrick analysis. All graphs were created using Origin 7.5.

LC-MS^n. The LC equipment (Agilent 1100 series, Bremen, Germany) comprised a binary pump, an autosampler with a 100 μL loop, and a DAD detector with a light-pipe flow cell (recording at 320 and 254 nm and scanning from 200 to 600 nm). This was interfaced with an ion trap mass spectrometer fitted with an ESI source (Bruker Daltonics HCT Ultra, Bremen, Germany) operating in Auto MS^n mode to obtain fragment ion m/z. As necessary, MS^2, MS^3, and MS^4 fragment-targeted experiments were performed to focus only on compounds producing parent ions at m/z 143, 161, 179, 197, 287, 305, 323, 341, 359, 449, 431, 467, 485, 503, 521, 611, 629, 647, 665, 683, 773, 791, 809, 827, and 845 in negative ion mode. Tandem mass spectra were acquired in Auto-MS^n mode (smart fragmentation) using a ramping of the collision energy. Maximum fragmentation amplitude was set to 1 V, starting at 30% and ending at 200%. MS operating conditions (negative mode) have been optimized using glucose with a capillary temperature of 365 °C, a dry gas flow rate of 10 L/min, and a nebulizer pressure of 12 psi.

HPLC. Separation was achieved on a 250 × 4.6 mm i.d. column containing diphenyl 5 μm and a 5 × 4.6 mm i.d. guard column of the same material (Varian, Darmstadt, Germany). Solvent (water/formic acid 1000:0.05 v/v) was delivered at a total flow rate of 850 μL/min by 25 min isocratic.

MALDI-TOF-MS. All experiments were performed in positive ion mode using an Ultraflex II MALDI TOF/TOF mass spectrometer (Bruker Daltonics) equipped with a pulsed 50 Hz N_2 laser (wavelength = 337 nm) and controlled by the FlexControl 3.0. software package (Bruker Daltonics). Laser intensity was varied in the range from 30 to 45%. Samples (0.5 μL) were deposed on top of a layer of crystals of 2,5-dihydroxybenzoic acid (DHB) formed by decomposition of 0.5 μL of DHB solution on the MALDI plate and allowing it dry at ambient temperature. A MALDI matrix was prepared by dissolving 5 mg of DHB in a 1 mL mixture of acetonitrile/methanol/aqueous trifluoroacetic acid (1%, v/v) (1:1:1, v/v/v). The MS/MS experiments were carried out using the LIFT method.

Thermogravimetric Analysis (TGA). TGAs were performed using a TA SDT Q600 instrument. The temperature was ramped from 25 to 180 °C for glucose and to 220 °C for starch and cellulose at a rate of 5 °C/min and kept at final temperature for 2 h using a nitrogen atmosphere.

Infrared (IR) Analysis. Infrared spectra were recorded on KBr pellets using a Nicolet Avatar 370 spectrometer.

^{1}H NMR and ^{13}C NMR. ^{1}H and ^{13}C NMR spectra were acquired on a JEOL ECX-400 spectrometer at room temperature in D_2O, using a 5 mm probe, operating at 400 and 100 MHz, respectively. The chemical shifts (δ) are reported in parts per million (ppm).

RESULTS AND DISCUSSION

For our investigations into the thermal decomposition of polysaccharides in food we chose starch and cellulose as the most relevant dietary polymers as model systems, although many other polysaccharides are found in foods such as glycogen in meat or arabinogalactans and galactomannans in coffee. In addition, we compared the data obtained with those of thermally treated glucose as a benchmark, the data of which have been discussed in detail previously.[12] If available data on the thermodegradation of starch and cellulose, differing by the stereochemistry of the 1,4-glycosidic linkage, are compared, no clear picture regarding their relative stabilities emerges. Whereas Alvarez et al.[19] reported a higher thermal stability for cellulose determined by TGA measurements (starch exothermic at 300 °C and cellulose at 320 °C), Aggarwal et al.[20] reported the opposite behavior, determining the activation energies for decomposition at values of 474 kJ/mol for starch and 242 kJ/mol for cellulose, indicating a higher stability for starch. The actual products of starch and cellulose thermal degradation have been investigated on two occasions by Zhang et al.[21] using solid state ^{13}C NMR spectroscopy, identifying ether linkages and carbonyls formed after dehydration at 300 °C, and by Hakkarainen using solid phase extraction followed by GC-MS analysis,[22] identifying 138 distinct products after heating to 230 °C and only 40 after heating to 190 °C, with aldehydes and ketones such as pentanal and pentanone, dicarboxylic acids, and γ-butyrolactone as the main volatile

dx.doi.org/10.1021/jf302135k | J. Agric. Food Chem. 2013, 61, 674–684

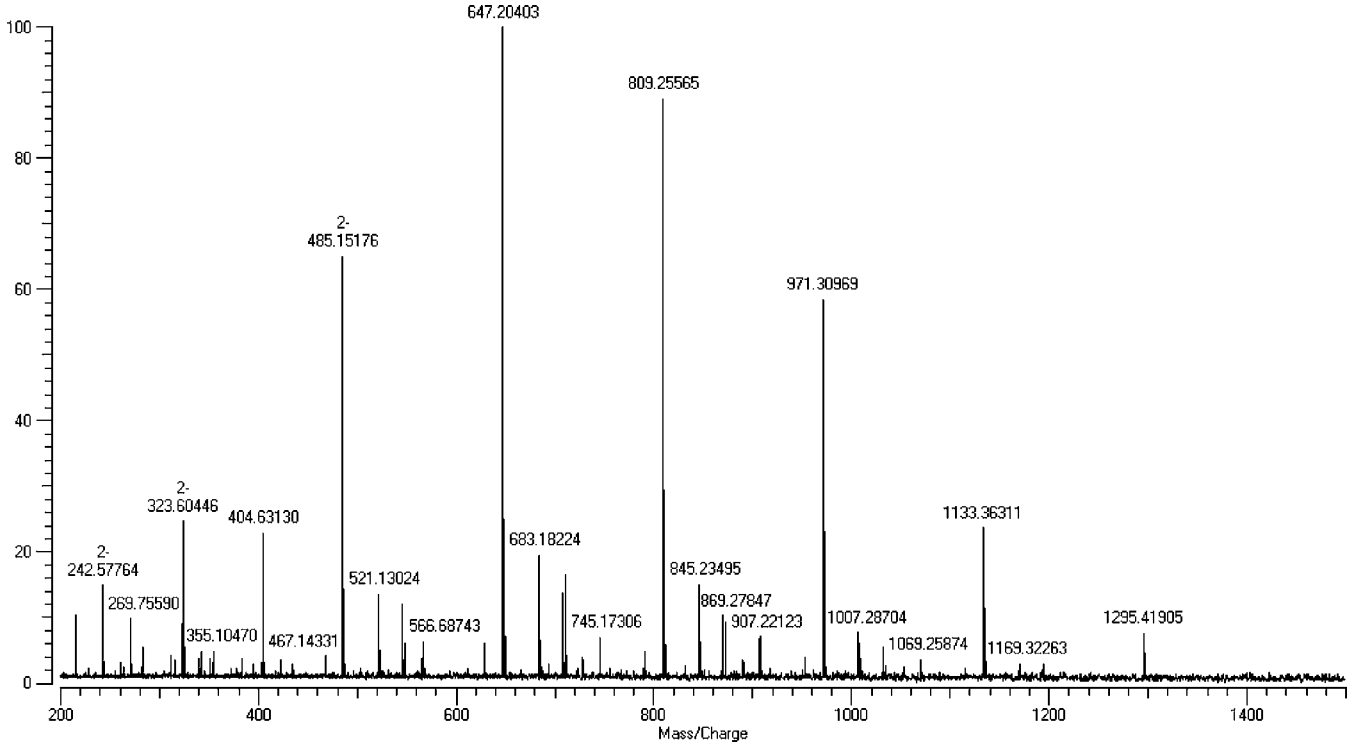

Figure 1. Mass spectrum of heated starch in negative ion mode using direct infusion into an ESI-FT-ICR instrument.

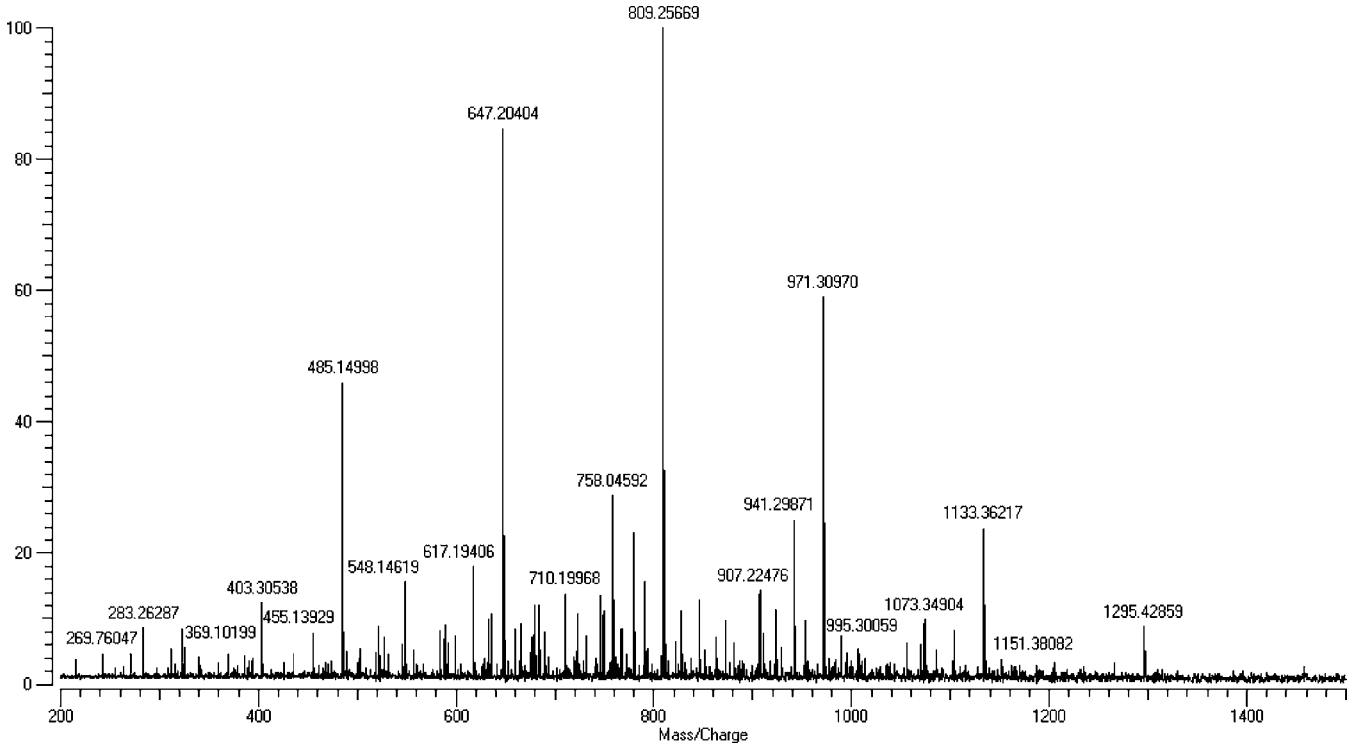

Figure 2. Mass spectrum of heated cellulose in negative ion mode using direct infusion into an ESI-FT-ICR instrument.

products. To the best of our knowledge no data exist on the nonvolatile fraction at temperatures typically employed in food processing.

To start our investigation, we acquired data from TGA for glucose, starch, and cellulose. All samples were heated from ambient temperature to 180 °C (glucose) and 220 °C (for starch and cellulose) and were kept for 2 h at these temperatures. Thermogravimetric curves of glucose and polysaccharides exhibited during this time span around 10–12% weight loss, which statistically corresponds to one water molecule per monosaccharide moiety, yet with slightly different patterns (see the Supporting Information). Gradual mass reduction was observed for polysaccharides, whereas for glucose, weight loss starts at higher temperature, compared to

dx.doi.org/10.1021/jf302135k | J. Agric. Food Chem. 2013, 61, 674–684

Table 1. High-Resolution Mass (ESI-FT-ICR) Data of Heated Starch and Their Parent Ions $[M - H]^-$

peak	assignment	mol formula	exptl m/z $[M - H]^-$	theor m/z $[M - H]^-$	rel error (ppm)
1	$(Glu)_4 - H_2O$	$C_{24}H_{40}O_{20}$	323.0998[b]	323.0984	0.9
2	$(Glu)_6 - H_2O$	$C_{36}H_{60}O_{30}$	485.1518[b]	485.1512	6.3
3	$(Glu)_3$	$C_{18}H_{32}O_{16}$	503.1597[a]	503.1618	4.1
4	$(Glu)_4 - 3 \times H_2O$	$C_{24}H_{36}O_{18}$	611.1835[a]	611.1829	1.0
5	$(Glu)_4 - 2 \times H_2O$	$C_{24}H_{38}O_{19}$	629.1967	629.1935	0.5
6	$(Glu)_4 - H_2O$	$C_{24}H_{40}O_{20}$	647.2036[a]	647.2040	0.6
7	$(Glu)_5 - 2 \times H_2O$	$C_{30}H_{48}O_{24}$	791.2491	791.2463	0.4
8	$(Glu)_5 - H_2O$	$C_{30}H_{50}O_{25}$	809.2557	809.2568	8.6
9	$(Glu)_5$	$C_{30}H_{52}O_{26}$	827.2638[a]	827.2674	4.3
10	$(Glu)_6 - 2 \times H_2O$	$C_{36}H_{58}O_{29}$	953.3027[a]	953.2991	3.8
11	$(Glu)_6 - H_2O$	$C_{36}H_{60}O_{30}$	971.3097	971.3097	5.6
12	$(Glu)_6$	$C_{36}H_{62}O_{31}$	989.3198[a]	989.3202	0.5
13	$(Glu)_7 - H_2O$	$C_{42}H_{70}O_{35}$	1133.3631	1133.3631	0.1
14	$(Glu)_8 - H_2O$	$C_{48}H_{80}O_{40}$	1295.4191	1295.4196	0.2

[a]From TOF-MS because of mass accuracy. [b]Doubly charged ion.

the two polysaccharides. The enhancement of temperature showed a comparable reduction of mass for starch and cellulose, and their TGA curves were observed to be identical.

Using this information, optimized temperature conditions were chosen, based on 10% weight loss, color formation (a visible degree of browning was observed), and recorded mass spectra of samples heated at different temperatures showing an abundance of product signals. In fact, 2 h at 180 °C for glucose and at 220 °C for starch and cellulose turned out to be the heating parameters used in all further studies. These heating conditions are similar to those employed in typical bread baking (220−240 °C for 60−100 min). The observation of the brown color of heated samples suggested that the caramelization process occurred in a manner similar to that for the roasting procedure of coffee beans or the heating of sugar food products.[23]

The thermal degradation products were hence dissolved in water and filtered. The weight percentage of the water-soluble fraction was 62% for starch, 23% for cellulose, and 100% for glucose. It is worth noting that both polymeric cellulose and starch in its granular form display poor water solubility.

In the following sections we will present and discuss data according to the work-flow of domino tandem mass spectrometry. We will start with a description of high-resolution MS data followed by application of chemometric tools. In a second consecutive step we will discuss analysis and structure elucidation for selected examples of hypothetical structures derived from the first part using LC-tandem MS. Finally, we apply our findings to the investigation of toasted bread.

Electrospray Fourier Transform Ion Cyclotrone Resonance (ESI-FT-ICR) Mass Spectrometry. As a first step ESI-FT-ICR mass spectra were acquired in both negative and positive ion modes for heated starch (**1**) and cellulose (**2**). Mass spectra for heated starch and cellulose in negative ion mode are shown in Figures 1 and 2, respectively. The positive ion mass spectra were dominated by sodiated molecular ions. Table 1 illustrates the mass/charge ratio (m/z) of the product ions, elemental composition, and average mass error for heated starch as the representative saccharide in negative ion mode. An inspection of the mass spectra showed the presence of oligomeric structures of glucose tetramer, pentamer, and hexamer **8** at m/z 665, 827, and 989. Oligomers of dehydrated glucose at m/z 647, 809, 971, 1133, and 1295 dominated the spectra. Dehydrated tetrameric **4** and hexameric **6** glucose appeared at m/z 323 and 485 as doubly negative charged ions, respectively (Figure 3). Further dehydration products arising

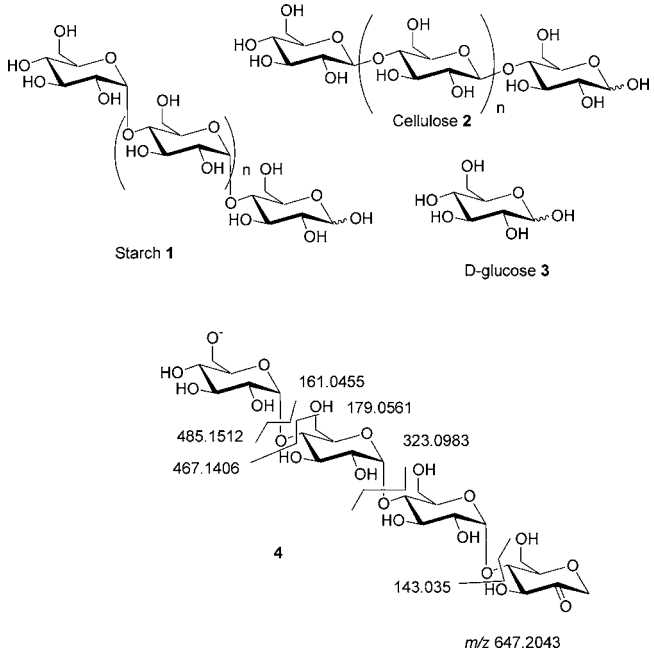

Figure 3. Chemical structures of starch, cellulose and D-glucose and fragmentation pattern observed for dehydrated tetramer of glucose **4** by IRMPD-FT-ICR-MS measurement.

from multiple water loss, including dehydration of monomeric carbohydrates and their oligomers demonstrating successive loss of up to eight water molecules, were observed. Interestingly, the thermal breakdown of both starch and cellulose leads to oligomers of glucose with a minimum number of four glucose moieties. No smaller oligomers were observed.

Signals displaying the nominal mass of hydration products were observed similar to those found in caramelized glucose; however, a close inspection of the accurate mass values in the case of starch and cellulose shows that these signals originate from ions with a different molecular formula (see the Supporting Information) and are assigned as condensed heterocyclic structures.

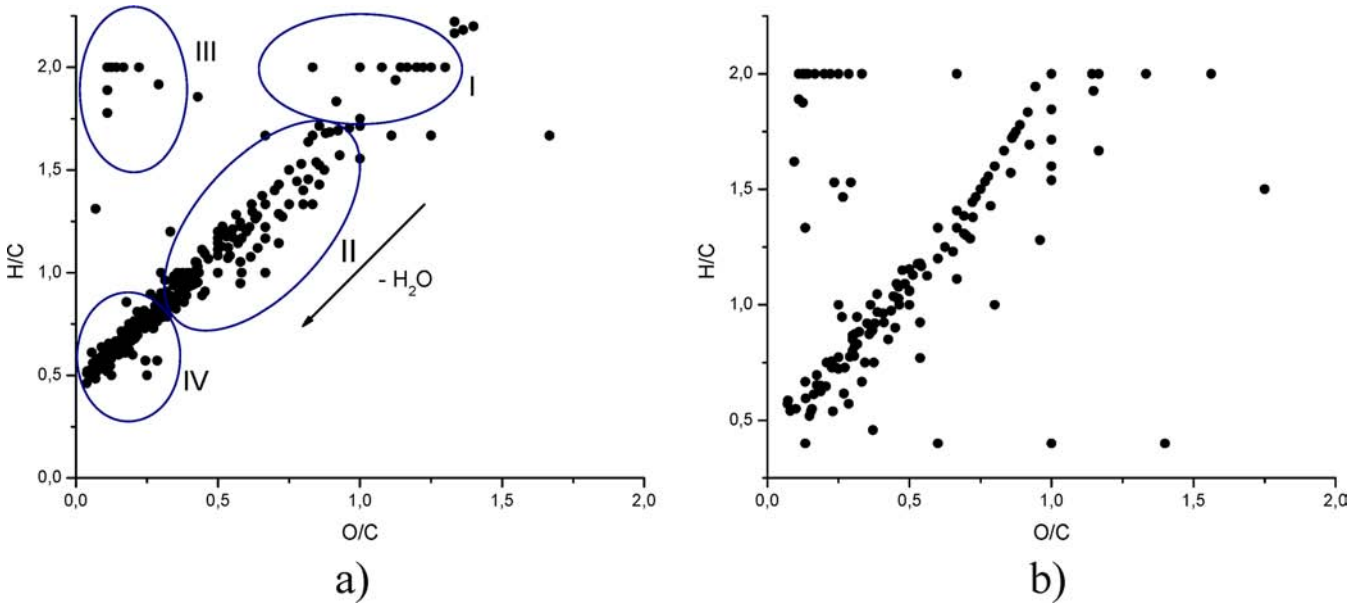

Figure 4. Two-dimensional van Krevelen plots (elemental ratio plot) showing the O/C ratio versus H/C ratio of heated (a) starch and (b) cellulose in negative ion mode in the m/z range between 50 and 1200.

The mass spectra of the thermal degradation products of starch and cellulose are remarkably similar, however showing the following subtle differences. The ion at m/z 683.18224, which corresponds to $C_{30}H_{36}O_{18}$ in negative ion mode, is observed only in the spectrum of starch, whereas the ion at m/z 941.29871 ($C_{35}H_{58}O_{29}$; $Glc_6 - C_1 - 2H_2O$) is found for cellulose. Both ions can be used as analytical markers indicating the presence of thermally treated starch or cellulose, respectively.

Chemometric Data Interpretation. We aim to characterize the nature of compounds formed during the heating procedure of the aforementioned carbohydrates. We applied novel mass spectrometric data interpretation strategies, such as van Krevelen and Kendrick plot analyses, to visualize the complex data, to give a general overview of all products of the heated carbohydrates, and to use as an inspiration for the further characterization of groups of compounds. The van Krevelen and Kendrick analyses have been on rare occasions employed for dietary materials, such as wine,[25] black tea thearubigins,[26] and caramel.[12] Therefore, in this study we applied these methods for the first time to heated polysaccharides. A general chemical reaction such as dehydration, reduction, or oxidation involves changes in the atomic ratios of O/C and H/C, and consequently some classes of compounds are characterized by a defined location on the graph, for instance, carbohydrates with typical atomic ratios (H/C ~ 2 and O/C ~ 1).[27] The van Krevelen plots generated from experimental high-resolution MS data for heated **1** and **2**, shown in Figure 4, have been annotated according to the class of products formed in the thermal decomposition reactions. In general, the profile of all graphs is similar to the predominant visible trend of the dehydration process for the group of points in the middle of the graph (II) and the group of points of carbohydrates in the upper right corner (I). The group of points is present in the upper left corner (III) with a significant deficiency in O among the molecules, probably due to the formation of disproportional redox reaction products. The next group of points in the bottom left corner with a significant deficiency in H indicates presumably the presence of condensed heterocyclic ring structures (IV). Only a limited number of points appears after point 1 in the O/C ratio and 2 in the H/C, which indicates that reduction instead of oxidation is a preferential process and dehydrogenation instead of hydrogenation during heating of carbohydrates.

The second graphical technique, which we applied to study the composition of heated polysaccharides, was the Kendrick plot, which allows identification of homologous series of compounds, differing by a predefined mass increment. The Kendrick plot is constructed using the values of Kendrick mass defect versus nominal Kendrick mass, derived from the conversion of high-resolution mass data from TOF-MS experiment into the Kendrick scale. To afford the Kendrick mass, the IUPAC mass of the compound is multiplied by 0.999413399, originating from 18/18.010565 for a water molecule. The nominal Kendrick mass (NKM) is defined as the Kendrick mass rounded to the nearest integer. The Kendrick mass defect (KMD) is defined as the difference between the exact Kendrick mass and the NKM.[28] If compounds belong to the same homologous series, they would have an identical Kendrick mass defect and lie on the horizontal lines in the graphs.[29] For our purpose, Kendrick plots were constructed with H_2O increment, and the graph for starch is shown in Figure 5. The graphs for all heated samples showed the presence of homologous series of the compounds with increment of water molecules indicating the presence of oligomers with up to five monomeric glucoses in the case of heated glucose and up to six glucoses in the case of heated polysaccharides, showing consecutive loss of up to eight water units. We used different colors to represent the groups of polymers; green represents monomers; gray, dimers; red, trimers; violet, tetramers; and blue, pentamers. Two novel high-resolution mass data interpretation techniques showed the whole range of products and reactions during the heating procedure of polysaccharides and their monomeric glucose. The further investigation was focused on the characterization of predominant products of the thermal treatment of the studied carbohydrates. Tandem MS and tandem MS coupled to liquid chromatography data for heated polysaccharides were acquired,

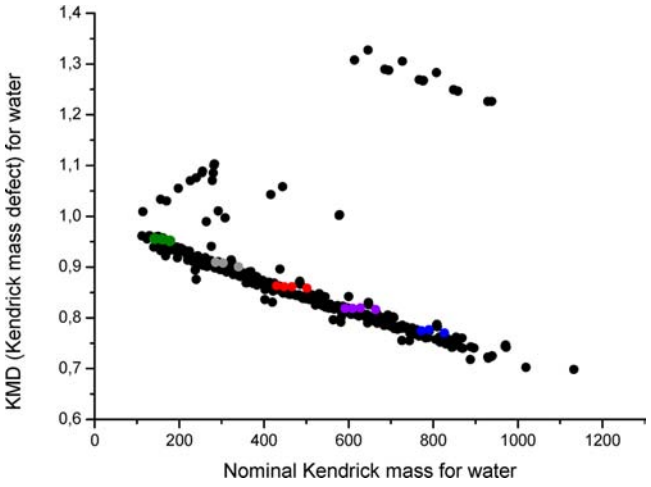

Figure 5. Two-dimensional Kendrick plot for mass increment H_2O showing the distribution of the Kendrick mass defect plotted against the nominal Kendrick mass of pseudomolecular ions for starch in negative ion mode. Colored data points parallel to the *x*-axis indicate homologous dehydration series.

analyzed, and compared to data of their monomeric glucose to allow further structure elucidation combined with separation of isomeric products in the chromatographic dimension.[30]

Characterization of Oligomers of Glucose. The MS^n data of monomeric glucose and their oligomers under heating of **1**, **2**, and **3** have been acquired in negative ion mode using a direct infusion into an ESI ion-trap mass spectrometer. The mass spectra of the fragment ion 179.0 monomers of glucose in the negative ion mode showed a loss of 18 as the main peak of **1** and **2** and a loss of 90 as the main peak of **3**, which corresponds to a water molecule and three formaldehyde molecules derived from the cross-ring cleavage, respectively. Glucose pentamers and hexamers **8** appeared at *m/z* 827 and 989. Fragmentation of tetrameric ion at *m/z* 341 (note it is the dimeric ion for **3**) gave different main peaks for all studied samples. The base fragment at *m/z* 179.0 is detected for **3** formed by the glycosidic bond cleavage between two monosacharides and may occur at either the reducing or nonreducing end, whereas the main peak at *m/z* 323 present for **1** and **2** corresponds to a dimer without one water molecule. MS^2 spectra of the ion at *m/z* 503 showed the main fragment ion at *m/z* 341 for glucose and at *m/z* 485 for starch and cellulose, derived from the glycosidic bond cleavage on the nonreducing end and dehydration of the precursor ion, respectively. MS^2 fragmentation of the ion at *m/z* 665, tetramer of glucose, gave predominant ions at *m/z* 503 for glucose and at *m/z* 647 for starch, indicating the cleavage of the glycosidic bond on nonreducing end and dehydration, respectively. Fragmentation of tetrameric ion of cellulose was not possible due to the low intensity. MS^2 spectra of the ion *m/z* 827 exhibited the main fragment ion at *m/z* 809 for starch and cellulose with a neutral loss of 18 (H_2O). The base peak at *m/z* 665, attributed to the pentamer of glucose, is present in the MS^2 spectrum of heated glucose and came from glycosidic bond cleavage on the nonreducing end, as observed for the aforementioned tetramers. MS^2 spectra of *m/z* 989, a hexamer of glucose, provided a base peak at *m/z* 827, from glycosidic bond cleavage at the nonreducing end for glucose, and at *m/z* 971 in the case of starch and cellulose. The predominant fragmentation pathway for glucose's oligomers of heated glucose involves cleavages of glycosidic bonds at the nonreducing end of the molecules. Fragmentation data of oligomers of glucose for studied polysaccharides are consistent with dehydration in the product ions. ESI-LC-MS experiments using the optimized chromatographic conditions for all heated carbohydrates were carried out. The extracted ion chromatograms (EICs) were generated for all oligomers of glucose and

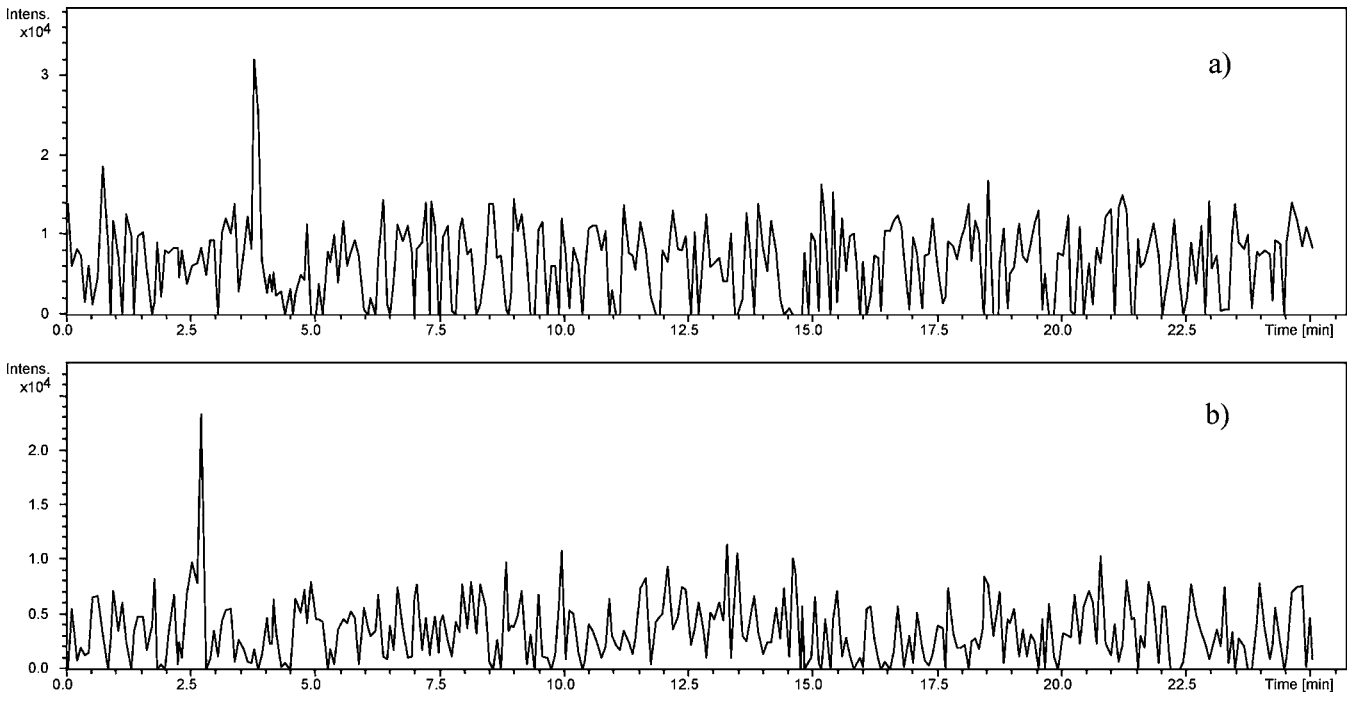

Figure 6. EICs of LC-MS of pseudomolecular ions at *m/z* (a) 665.0 ($C_{24}H_{42}O_{21}$) and (b) 647.0 ($C_{24}H_{40}O_{20}$) of heated cellulose in negative ion mode.

dx.doi.org/10.1021/jf302135k | J. Agric. Food Chem. 2013, 61, 674−684

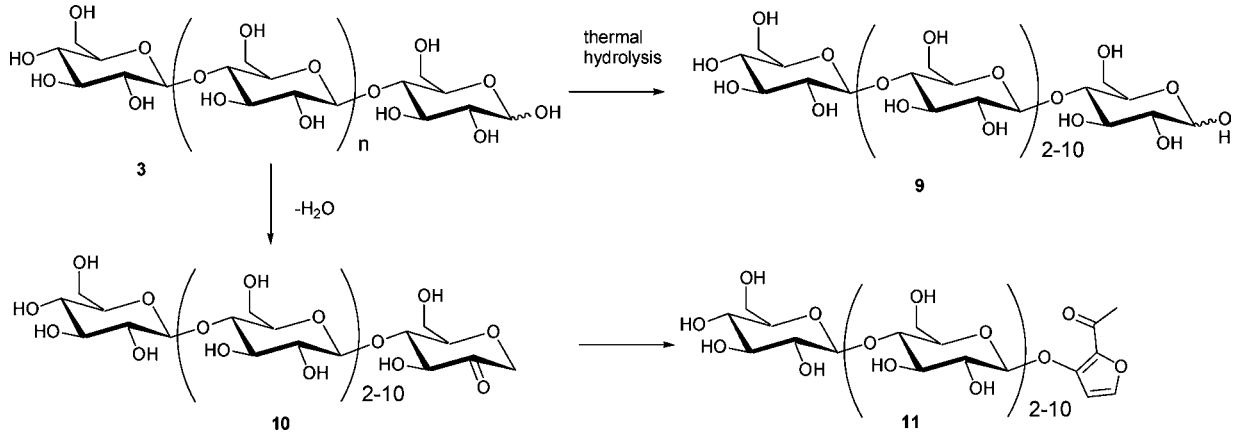

Figure 7. Reaction mechanism illustrating thermal decomposition of cellulose.

detected different numbers of chromatographic peaks. As an example, the EIC of the ion at m/z 665 of tetrameric glucose gave one chromatographic peak for heated cellulose (Figure 6). The presence of a single chromatographic peak suggested that chemoselective single site cleavages of the glycosidic bonds occur in starch and cellulose as opposed to glycosidic bond breaking to form monomeric glucose followed by reassembling through de novo glycosidic bond formation as observed for caramelized glucose. Multiple chromatographic peaks were observed for the tetramer of heated glucose, indicating the nonselective formation of numerous isomers.

Characterization of Dehydration Products. Dehydrated oligomers of glucose with dehydrated glucose were the predominant products of the thermal treatment of the studied carbohydrates, and all were visualized and hence assigned using van Krevelen and Kendrick mass analyses. Dehydrated oligomers of heated samples derived from a loss of a single water molecule were observed at m/z 323.1, 485.1, 647.2, and 809.2 with dehydrated monomer of glucose at m/z 161.1 for glucose and at m/z 647.2, 809.2, 971.3, 1133.4, and 1295.4 for heated starch and cellulose. When a water molecule is eliminated from glucose at C1−C4 positions, an enol is formed, which tautomerizes to its carbonyl form (Figure 7). NMR and IR data analyses of all heated samples supported the presence of such carbonyl groups. Alternatively, the formation of a 1,6-anhydroglucose at the reducing terminus must be considered.

To compare the structure and fragmentation behavior of the dehydrated oligomers of glucose, an infrared multiple photon dissociation (IRMPD) experiment was carried out on a selected precursor ion at m/z 647 of a dehydrated tetramer with the empirical molecular formula $C_{24}H_{40}O_{20}$ **4** for both heated starch and cellulose. The spectra are shown in the Supporting Information and the fragment ions in Table 2. Major fragment ions are shown for the example of starch in Figure 3. Again, the fragment ions originating from starch and cellulose are remarkably similar, displaying the following subtle differences. Fragment ions unique for starch are present at m/z 467.14058, which correspond to didehydrated trimer with the molecular formula $C_{18}H_{28}O_{14}$ and ions at m/z 383.11701 ($C_{14}H_{24}O_{12}$) and 221.06659 ($C_8H_{13}O_7$), both originating from cross-ring cleavages. Unique peaks for cellulose are present at m/z 394.76693 and 254.85563. Moreover, the intensity of the fragment ion at m/z 179 differed for cellulose and starch, appearing at 30 and 50% intensities, respectively. Reinhold and co-workers noted that in fragmentation processes α-glycosidic linkages are more labile compared to β-glycosidic linkages observed in cellulose, which is in agreement with this observation.[24]

Table 2. MALDI-MS/MS Data in Positive Ion Mode of the Bread Sample (Presented Ions Are Sodiated Adducts)

m/z	assignment	MS^2 m/z (intensity)
527.0	$(Glu)_3$	85.2 (1%); 103.2 (5%); 123.9 (1%); 182.7 (9%); 201.8 (1%); 345.4 (4%); 363.4 (11%); 380.7 (1%); 465.4 (3%)
689.0	$(Glu)_4$	74.6 (2%); 331.8 (10%); 346.3 (2%); 354.2 (4%); 364.4 (3%); 508.4 (3%); 526.4 (6%)
1175.0	$(Glu)_7$	74.5 (19%); 346.8 (13%); 508.8 (18%); 526.8 (8%); 670.9 (16%); 688.9 (11%); 832.8 (7%); 850.9 (8%); 1013.2 (14%)
1157.0	$(Glu)_7 - H_2O$	70.0 (2%); 347.0 (9%); 509.1 (21%); 671.3 (22%); 833.4 (15%); 851.4 (2%); 995.7 (11%)
1319.0	$(Glu)_8 - H_2O$	104.0 (22%); 347.1 (40%); 509.2 (60%); 671.3 (60%); 833.4 (34%); 995.6 (22%); 1157.6 (19%)
1643.0	$(Glu)_{10} - H_2O$	74.1 (33%); 346.7 (26%); 508.6 (40%); 670.6 (41%); 832.7 (34%); 994.8 (22%); 1156.8 (14%); 1318.7 (14%); 1480.7 (18%)

To distinguish between these two alternatives of a carbonyl tautomer or 1,6-anhydroglucose as the dehydration products, we argue using the appearance of fragment ions at m/z 383.11701 and 221.06659 in the IRMPD tandem MS spectra of, for example, the tetrameric ion at m/z 647.20410 as the precursor ion (see Supporting Information S4). These two fragment ions can be rationalized only by assuming loss of one or two $C_6H_{10}O_5$ moieties followed by the loss of a $C_4O_3H_6$ moiety. The latter would require breakage of at least three covalent bonds in 1,6-anhydroglucose and therefore supports the structural alternative of a carbonyl tautomer. Fragmentation of monodehydrated trimers at m/z 485 furnished the main fragment at m/z 323 with a neutral loss of 162 ($C_6H_{10}O_5$) for all analyzed samples. MS^2 spectra of the ion m/z 647, the monodehydrated tetramer of glucose, showed the main peak at m/z 485, and it is consistent for all analyzed samples with a neutral loss of 162 ($C_6H_{10}O_5$). In comparison to the previously discussed IRMPD data of this precursor ion, the collision-induced dissociation (CID) obtained here revealed a smaller number of fragment ions as expected. Fragmentation of the monodehydrated pentamer at m/z 809 gave the main peaks at m/z 647 for all studied saccharides and excluded the cleavage of the glycosidic bond at the internal part of the molecule. Dehydration reaction products with two or more water

dx.doi.org/10.1021/jf302135k | J. Agric. Food Chem. 2013, 61, 674−684

molecules were observed for the studied oligomers of glucose of heated polysaccharides and glucose itself. Didehydrated ions of a trimer, tetramer and pentamer appeared at m/z 467.1, 629.2, and 791.2 in negative ion mode. The MS^2 spectra of an ion at m/z 467 exhibited for all studied samples the main fragment with a neutral loss of 18 (H_2O). Low intensities and MS^2 data are not discussed. Tridehydrated oligomers of glucoses appeared at m/z 287.1, 449.1, and 611.2. MS^2 spectra of the ion at m/z 287, a dimer after losing three water molecules, gave neutral losses of 126 ($C_6H_6O_3$) as the main fragments for **2** and **3**. This suggests the presence of isomaltol as suggested by Moreira et al.[23] or 5-hydroxymethylfurfural as observed in the tridehydration of glucose,[12] supporting the fact that elimination of all three water molecules appeared at one saccharide moiety. In the absence of a diagnostic fragment ion that could be further interrogated to be able to distinguish between isomaltol and its structural alternative, the nature of this moiety remains speculative. The main fragment ion for 287 of heated glucose appeared at m/z 238.7, whereas the ion with a neutral loss of 126 was present with an intensity around 20%. MS^2 spectra of the ion at m/z 449.1 provided the main peak at m/z 405 for **1** and **2** with a neutral loss of 44 (C_2H_4O), whereas for **3** the ion at m/z 431 showed a neutral loss of 18 (H_2O), although ions with neutral losses of 126 are present. MS^2 data of the tridehydrated tetramer at m/z 611 were recorded only for heated glucose and gave an ion at m/z 449 as the base peak. The ion of tridehydrated pentamer at m/z 773 fragmented and gave the main ion at m/z 611 for glucose and at m/z 755 for starch and cellulose, which derived from glycosidic bond cleavage at the nonreducing end and dehydration, respectively.

The EIC of the ion at m/z 647 of a dehydrated tetramer of glucose gave one chromatographic peak in the case of heated cellulose (Figure 6). This confirmed the extensive cleavage of the glycosidic bonds.

To visualize differences in ions observed in heated starch, cellulose, and glucose, radar plots were created to show the intensities of various ions on the apexes of the plot with all three different samples given as lines of different colors (Figure 8). The first graph illustrates the differences in intensities of monomeric and oligomeric ions. We found out that the formation of oligomers in the case of glucose appeared in a similar manner as the degradation of polysaccharides. Cellulose degrades preferentially in comparison with starch. The second chart shows differences in intensities of dehydrated products. The formation of dehydrated oligomers occurs predominately in the order starch > cellulose > glucose. On the other hand, monomeric glucose forms dehydrated products first and starch and cellulose in a similar manner. Finally, the third plot describes the ratios of intensities of oligomers to dehydrated oligomers. Glucose differs from polysaccharides with lower degrees of dehydration, and it is followed by cellulose and starch.

MALDI-MS Analysis of Thermally Treated Glucose and Polysaccharides. MALDI-MS analysis with DHB as a matrix was performed for heated polysaccharides and glucose (Figure 9). In addition to mass spectra recorded with the ESI technique, high molecular weight oligosaccharides were observed up to undecamers in the case of glucose and up to dodecamers for starch and cellulose (see Figures 7 and 10). We observed ions at m/z 527, 689, 851, 1013, 1175, 1337, 1499, 1661, and 1823 in positive ion mode attributed to sodiated adducts of oligomeric glucoses up to undecamers. MALDI-MS spectra of heated starch and cellulose showed the presence of

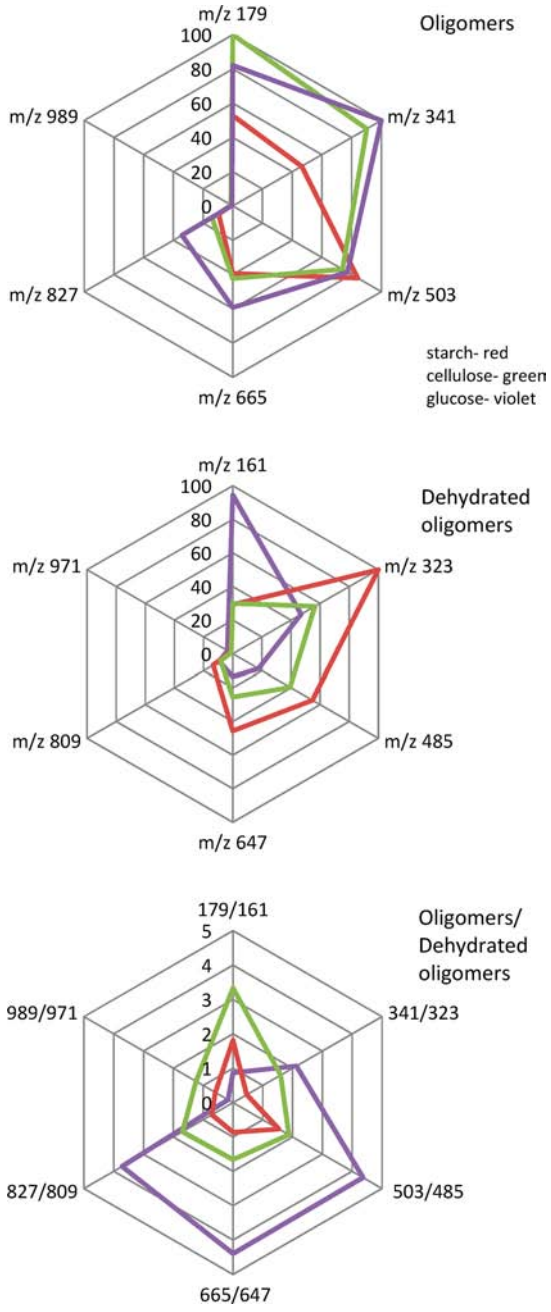

Figure 8. Radar plots of different product ions observed for heated starch, cellulose, and glucose.

the most intense ions at m/z 347, 509, 671, 833, 995, 1157, 1319, 1481, 1643, 1805, and 1967, corresponding to dehydratated sodiated adducts of oligomers up to dodecamers. The observation of ions with increased m/z ratios indicates again the utility of MALDI-MS to cover an extended mass range in carbohydrate analysis. Similar products were observed in intact wood tissues by Yost et al.[31] The MALDI-MS data confirmed the polymerization process of glucose, the depolymerization of polysaccharides, and the formation of dehydrated derivatives of all saccharides afforded by ESI-MS. Moreover, MS^2 spectra of oligomers and dehydrated oligomer ions of heated samples have been recorded and are presented in the Supporting Information. The tandem MALDI-MS/MS data confirm the identity of structures of ions observed in MALDI-MS if compared to those observed by ESI-MS.

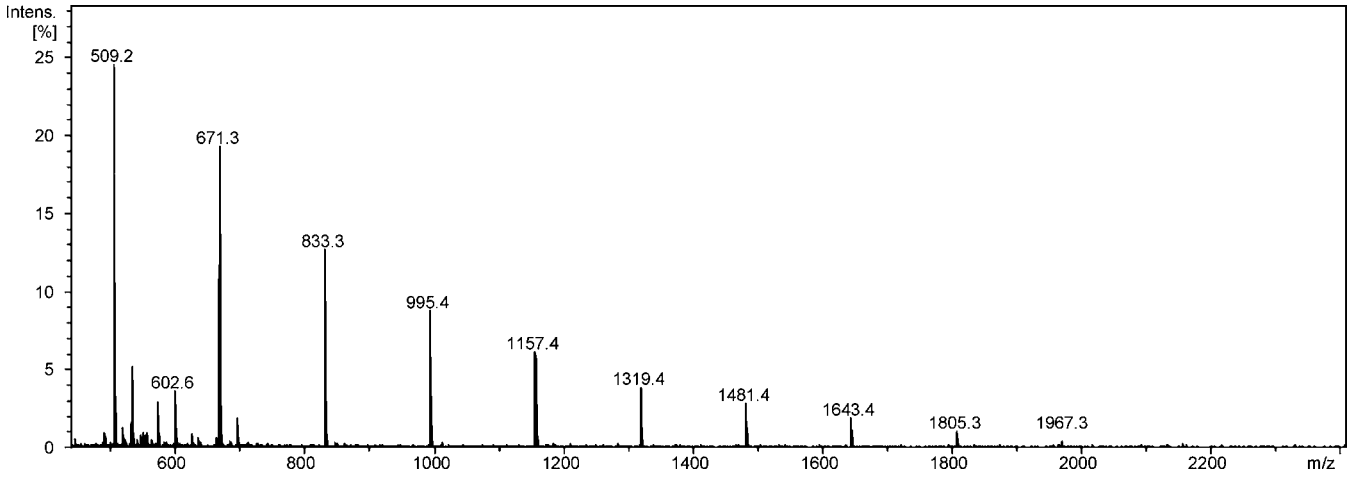

Figure 9. Mass spectrum of heated starch in positive ion mode using the MALDI-TOF-MS instrument.

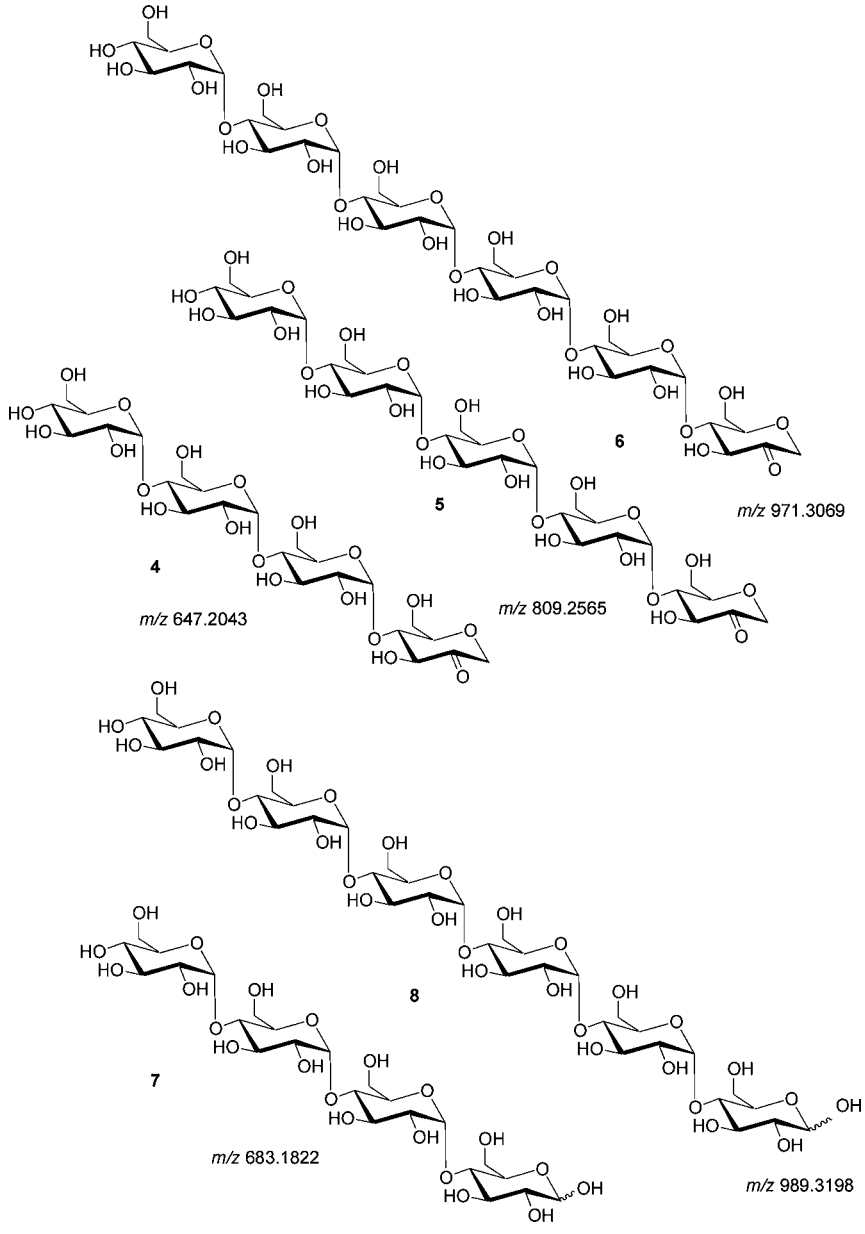

Figure 10. Structures of oligomeric and dehydrated oligomeric decomposition products **4**–**8** obtained from starch.

dx.doi.org/10.1021/jf302135k | *J. Agric. Food Chem.* 2013, 61, 674–684

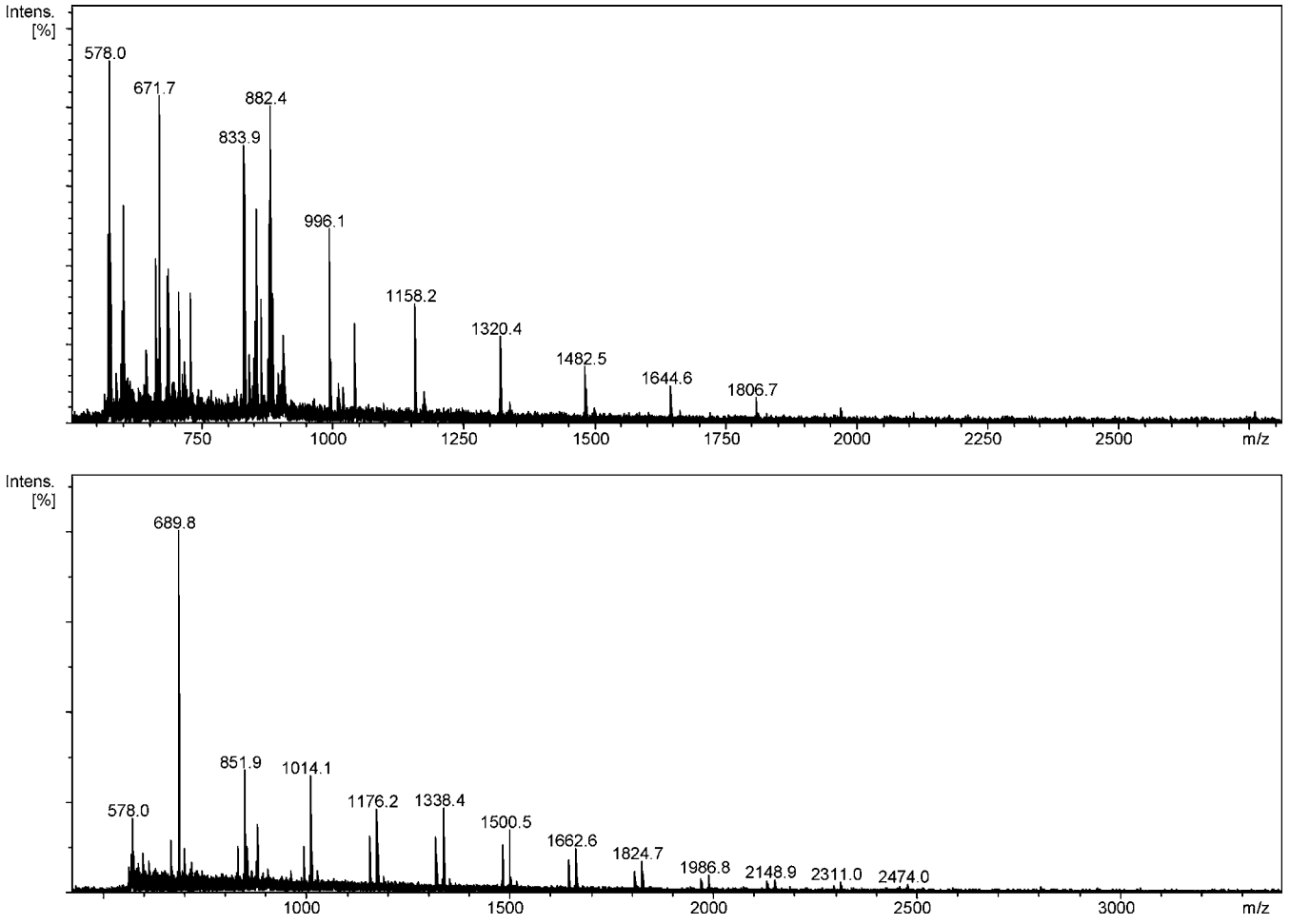

Figure 11. Mass spectra of baked bread in positive ion mode using the MALDI-TOF-MS instrument.

Analysis of Polysaccharide Thermal Degradation Products in Bread. Baked bread is one of mankind's oldest foods. Archeological findings in Göbekli Tepe in southeastern Turkey from the Neolithic period 9000 BC have provided evidence for the first use of wheat, following a genetic mutation of wheat to produce a shattering rachis in that region, in breadmaking. Definite evidence of baking bread originates from a scene in the tomb of Ramses III displaying the pharaonic bakery producing bread and cakes. Polysaccharides are the main components of bread, and white bread contains 42.5% of starch and 1.5% of cellulose.[32,33]

To provide insight into the chemistry involved in bread baking and relate the findings to the model systems studied above, we investigated the carbohydrate fraction of baked bread.

Using a simple extraction procedure of wheat-based bread heated in the toaster followed by an ESI-TOF-MS experiment resulted in extremely complex spectra not enable to further interpretation. The use of MALDI-TOF-MS, however, provided clean spectra that were dominated by signals corresponding to oligomeric carbohydrates. It is worth noting that ions appeared as sodiated and sometimes sodiated and protonated ions in positive ion mode.

Two representative spectra are shown in Figure 11. High molecular weight oligosaccharides were observed up to undecamers. We furthermore observed ions at *m/z* 527, 689, 851, 1013, 1175, 1337, 1499, 1661, and 1823 in positive ion mode attributed to sodiated adducts of oligomeric glucoses up to dodecamers. MALDI-MS spectra of toasted bread extracts showed the presence of the most intense ions at *m/z* 347, 509, 671, 833, 995, 1157, 1319, 1481, 1643, 1805, and 1967, corresponding to dehydratated sodiated adducts of oligomers up to dodecamers, similar to the starch model system, indicating that the identical thermal degradation processes occurring in the model systems did as well take place in bread thermal processing. Table 2 presents the fragment ions of three oligomeric carbohydrates and dehydrated oligomeric carbohydrates. The main fragmentation pattern involves cleavages of glycosidic bonds, which additionally prove the identity of the compounds present in bread.

■ ASSOCIATED CONTENT

Supporting Information

Additional EICs, MS^2 + MS^3 data of all compounds mentioned in the text, table of high-resolution MS-TOF data for compounds identified, and NMR and IR spectra. This material is available free of charge via the Internet at http://pubs.acs.org.

■ AUTHOR INFORMATION

Corresponding Author

*Phone: 49 421 200 3120. Fax: 49 421 200 3229. E-mail: n.kuhnert@jacobs-university.de.

Funding

We thank Jacobs Universtiy Bremen and the Fond für Angewandte Umweltforschung des Landes Bremen for funding. F.J.G. and J.Z.D. gratefully acknowledge the support of the Spanish Project MICINN/CTQ 2009-13652.

Notes

The authors declare no competing financial interest.

■ ACKNOWLEDGMENTS

We gratefully acknowledge technical assistance by Anja Müller.

■ REFERENCES

(1) Simões, J.; Domingues, P.; Reis, A.; Nunes, F. M.; Coimbra, M. A.; Domingues, M. R. M. Identification of anomeric configuration of underivatized reducing glucopyranosyl-glucose disaccharides by tandem mass spectrometry and multivariate analysis. *Anal. Chem.* **2007**, *79*, 5896−5905.

(2) Hernández-Hernández, O.; Ruiz-Aceituno, L.; Sanz, M. L.; Martínez-Castro, I. Determination of free inositols and other low molecular weight carbohydrates in vegetables. *J. Agric. Food Chem.* **2011**, *59*, 2451−2455.

(3) Deguchi, S.; Tsujii, K.; Horikoshi, K. Cooking cellulose in hot and compressed water. *Chem. Commun.* **2006**, 3293−3295.

(4) Siljeström, M.; Björck, I.; Westerlund, E. Transglycosidation reactions following heat treatment of starch − effects on enzymic digestibility. *Starch/Staerke* **1989**, *41*, 95−100.

(5) Singh, N.; Sing, J.; Kaur, L.; Sodhi, N. S.; Gill, B. S. Morphological, thermal and rheological properties of starches from different botanical sources. *Food Chem.* **2003**, *81*, 219−231.

(6) Pizzoferrrato, L.; Paci, M.; Rotilio, G. Structural modification and bioavailability of starch components as related to the extent of Maillard reaction: an enzymatic degradation and a solid-state ^{13}C CPMAS NMR study. *J. Agric. Food Chem.* **1998**, *46*, 438−441.

(7) Abdel-Aal, E.-S. M; Rabalski, I. Effect of baking on nutritional properties of starch in organic spelt whole grain products. *Food Chem.* **2008**, *111*, 150−156.

(8) Tizzotti, M. J.; Sweedman, M. C.; Tang, D.; Schaefer, Ch.; Gilbert, R. G. New ^{1}H NMR procedure for the characterization of native and modified food-grade starches. *J. Agric. Food Chem.* **2011**, *59*, 6913−6919.

(9) Fogliano, V.; Morales, F. J. Estimation of dietary intake of melanoidins from coffee and bread. *Food Funct.* **2011**, *2*, 117−123.

(10) Kuhnert, N.; Drynan, J. W.; Obuchowicz, J.; Clifford, M.; Witt, M. Mass spectrometric characterization of black tea thearubigins leading to an oxidative cascade hypothesis for thearubigin formation. *Rapid Commun. Mass Spetrom.* **2010**, *24*, 3387−3404.

(11) Jaiswal, R.; Matei, M. F.; Golon, A.; Witt, M.; Kuhnert, N. Understanding the fate of chlorogenic acids in coffee roasting using mass spectrometry based targeted and non-targeted analytical strategies. *Food Funct.* **2012**, *3*, 976−984.

(12) Golon, A.; Kuhnert, N. Unraveling the chemical composition of caramel. *J. Agric. Food Chem.* **2012**, *60* (12), 3266−3274.

(13) Wei, C.; Qin, F.; Zhou, W.; Xu, B.; Chen, Ch.; Chen, Y.; Wang, Y.; Gu, M.; Liu, Q. Comparison of the crystalline properties and structural changes of starches from high-amylose transgenic rice and its wild type during heating. *Food Chem.* **2011**, *128*, 645−652.

(14) Hurkman, W. J.; Wood, D. F. High temperature during grain fill alters the morphology of protein and starch deposits in the starchy endosperm cells of developing wheat (*Triticum aestivum* L.) grain. *J. Agric. Food Chem.* **2011**, *59*, 4938−4946.

(15) Dos-Santos, N.; Jiménez-Araujo, A.; Rodríguez-Arcos, R.; Fernández-Trujillo, J. P. Cell wall polysaccharides of near-isogenic lines of melon (*Cucumis melo* L.) and their inbred parentals which show differential flash firmness or physiological behavior. *J. Agric. Food Chem.* **2011**, *59*, 7773−7784.

(16) Matthews, J. F.; Bergenstråhle, M.; Beckham, G. T.; Himmel, M. E.; Nimlos, M. R.; Brady, J. W.; Crowley, M. F. High-temperature behavior of cellulose I. *J. Phys. Chem. B* **2011**, *115*, 2155−2166.

(17) Klemm, D.; Heublein, B.; Fink, H.-P.; Bohn, A. Cellulose: fascinating biopolymer and sustainable raw material. *Angew. Chem., Int. Ed.* **2005**, *44*, 3358−3393.

(18) Clowers, B. H.; Dodds, E. D.; Seipert, R. R.; Lebrilla, C. B. Dual polarity accurate mass calibration for electrospray ionization and matrix-assisted laser desorption/ionization mass spectrometry using maltooligosaccharides. *Anal. Biochem.* **2008**, *381*, 205−213.

(19) Alvarez, V. A.; Vázquez, A. Thermal degradation of cellulose derivatives/starch blends and sisal fibre biocomposites. *Polym. Degrad. Stab.* **2004**, *84*, 13−21.

(20) Aggarwal, P.; Dollimore, D.; Heon, K. Comparative thermal analysis study of two biopolymers, starch and cellulose. *J. Therm. Anal.* **1997**, *50*, 7−17.

(21) Zhang, X.; Golding, J.; Burgar, I. Thermal decomposition chemistry of starch studied by ^{13}C high-resolution solid-state NMR spectroscopy. *Polymer* **2002**, *43*, 5791−5796.

(22) Hakkarainen, M.; Albertsson, A. C.; Karlsson, S. Solid-phase extraction and subsequent gas chromatography-mass spectrometry analysis for identification of complex mixtures of degradation products in starch-based polymers. *J. Chromatogr., A* **1996**, *741*, 251−263.

(23) Moreira, A. S. P.; Coimbra, M. A.; Nunes, F. M.; Simões, J.; Domingues, M. R. M. Evaluation of the effect of roasting on the structure of coffee galactomannans using model oligosaccharides. *J. Agric. Food Chem.* **2011**, *59*, 10078−10087.

(24) Ashline, D.; Singh, S.; Hanneman, A.; Reinhold, V. Congruent strategies for carbohydrate sequencing. 1. Mining structural details by MS^n. *Anal. Chem.* **2005**, *77*, 6250−6262.

(25) Gougeon, R. D.; Lucio, M.; Frommberger, M.; Peyron, D.; Chassagne, D.; Alexandre, H.; Feuillat, F.; Voilley, A.; Cayot, P.; Gebefugi, I.; Hertkorn, N.; Schmitt-Kopplin, P. The chemodiversity of wines can reveal a metabologeography expression of cooperage oak wood. *Proc. Natl. Acad. Sci. U.S.A.* **2009**, *106*, 9174−9179.

(26) Kuhnert, N. Unraveling the structure of the black tea thearubigins. *Arch. Biochem. Biophys.* **2010**, *501*, 37−51.

(27) Hertkorn, N.; Frommberger, M.; Witt, M.; Koch, B. P.; Schmitt-Kopplin, P.; Perdue, E. M. Natural organic matter and the event horizon of mass spectrometry. *Anal. Chem.* **2008**, *80*, 8908−8919.

(28) Wu, Z.; Rodgers, R. P.; Marshall, A. G. Two- and three-dimensional van Krevelen diagrams: a graphical analysis complementary to the Kendrick mass plot for sorting elemental compositions of complex organic mixtures based on ultrahigh-resolution broadband Fourier transform ion cyclotron resonance mass measurements. *Anal. Chem.* **2004**, *76*, 2511−2516.

(29) Hughey, C. A.; Hendrickson, C. L.; Rodgers, R. P.; Marshall, A. G.; Qian, K. N. Kendrick mass defect spectrum: a compact visual analysis for ultrahigh-resolution broadband mass spectra. *Anal. Chem.* **2001**, *73*, 4676−4681.

(30) Kuhnert, N.; Clifford, M. N.; Müller, A. Oxidative cascade reactions yielding polyhydroxy-theaflavins and theacitrins in the formation of black tea thearubigins: evidence by tandem LC-MS. *Food Funct.* **2010**, *1*, 180−199.

(31) Lunsford, K. .A; Peter, G. F.; Yost, R. A. Direct matrix-assisted laser desorption/ionization mass spectrometric imaging of cellulose and hemicellulose in *Populus* tissue. *Anal. Chem.* **2011**, *83*, 6722−6730.

(32) Carpenter, T. M. Composition of some common foods with respect to the carbohydrate content. *J. Nutr.* **1940**, *19* (5), 415−422.

(33) Kuhnert, N.; Golon, A. Untersuchung von Karamel durch Domino Tandem Massenspektrometrie. *Dtsch. Lebensm. Rundsch.* **2012**, *23*, 345−349.